Preprints of the 23rd IFAC World Congress
Busan, Republic of Korea, August 23-28, 2026

Distributed Traffic Signal Control of Interconnected Intersections: A Two-Lane Traffic Network Model ⋆

Xinfeng Ru *,***, **Ting Bai** **, **Weiguo Xia** *, **Dongdong Qin** ***, **and Andreas A. Malikopoulos** ****

* *Key Laboratory of Intelligent Control and Optimization for Industrial Equipment of Ministry of Education, and School of Control Science and Engineering, Dalian University of Technology, Dalian, China (e-mails: rxf@mail.dlut.edu.cn, wgxiaseu@dlut.edu.cn).*
** *School of Automation and Intelligent Sensing, Shanghai Jiao Tong University, Shanghai, China (e-mail: tingbai@sjtu.edu.cn).*
*** *East China University of Science and Technology, Shanghai, China (e-mail:ddq@ecust.edu.cn).*
**** *Information and Decision Science Lab, School of Civil & Environmental Engineering, Cornell University, New York, USA(e-mails: tingbai@cornell.edu, amaliko@cornell.edu).*

Abstract: In this paper, we investigate traffic signal control in a network of interconnected intersections, aiming to balance lane-level vehicle densities through optimal green-time allocation. We develop a two-lane traffic flow model that explicitly captures lane-specific propagation dynamics, addressing key limitations of conventional road-level formulations. The proposed model offers a more granular and flexible representation of urban traffic, enabling controllers to react more accurately to lane-specific congestion patterns. Building on this model, we design a distributed model predictive control (MPC) framework and integrate it with the efficient alternating direction method of multipliers (ADMM) to enhance scalability and real-time performance. To accommodate time-varying traffic conditions, we further introduce a data-driven method for forecasting dynamic split ratios. Comprehensive VISSIM simulations on a six-intersection network in Dalian, China, demonstrate that the proposed approach outperforms existing signal control strategies in both traffic efficiency and computational speed, showing its promise for real-time deployment.

Keywords: Traffic network model, traffic signal control, distributed MPC, ADMM.

1. INTRODUCTION

Traffic congestion has become a pressing global challenge due to the rapid growth of vehicle populations and the limited expandability of urban infrastructure. To mitigate congestion, several control strategies have been studied, including signal offset control for green-wave progression (De Nunzio et al., 2015), route planning and optimization (Ba et al., 2015; Bai et al., 2025; Li et al., 2025; Bang et al., 2022), and green-time allocation for traffic regulation (Grandinetti et al., 2018; Ru et al., 2023). Among them, green-time allocation is particularly attractive because it is scalable and compatible with existing traffic infrastructure.

Traditional traffic models usually aggregate multiple lanes of a road into a single state variable. Based on such road-level models, fixed-time methods (Robertson, 1969), adaptive systems such as SCOOT (Robertson and Bretherton, 1991) and SCATS (Sims and Dobinson, 1980), and distributed MPC approaches (Camponogara and De Oliveira, 2009; Grandinetti et al., 2018) have been developed for signal control. Model-free adaptive predictive control (Ru et al., 2023) and max-pressure control (Zaidi et al., 2016) have also been investigated to improve traffic efficiency. However, these approaches generally overlook lane-specific congestion patterns and turning behaviors.

Recent studies on connected and automated vehicles have further highlighted the importance of fine-grained modeling and predictive decision-making in urban traffic systems (Malikopoulos et al., 2021; Chalaki and Malikopoulos, 2021; Tzortzoglou et al., 2024; Bai et al., 2023; Chalaki and Malikopoulos, 2022; Le and Malikopoulos, 2024). Nevertheless, most existing signal control methods still rely on aggregated road-level models, implicitly assuming that vehicles are evenly distributed across lanes. Although split ratios have been introduced to approximate lane usage (De Oliveira and Camponogara, 2010; Yan et al., 2016), they are often treated as fixed parameters and therefore cannot capture time-varying turning behaviors.

⋆ This work was supported in part by the National Natural Science Foundation of China under Grant 62122016, NSF under Grants CNS-2401007, CMMI-234881, IIS-2415478, MathWorks, and the Research Start-Up Fund from Shanghai Jiao Tong University under Grant WL220203203.

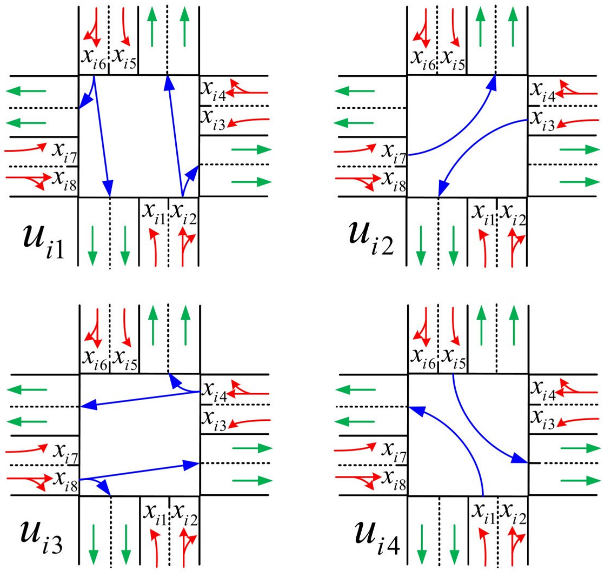

Fig. 1. Illustration of a four-way intersection i, where lanes x_{i2} and x_{i6} are controlled by input u_{i1}; lanes x_{i3} and x_{i7} by u_{i2}; lanes x_{i4} and x_{i8} by u_{i3}; and lanes x_{i1} and x_{i5} by u_{i4}.

To address these limitations, we develop a two-lane traffic model that explicitly incorporates lane-level vehicle dynamics and turning movements. Each road is modeled by two parallel lanes, and four signal phases at each intersection regulate the corresponding lane-level discharge flows, as illustrated in Fig. 1. Building on this model, we propose a distributed MPC framework for dynamic green-time allocation across interconnected intersections. To improve scalability and real-time feasibility, the alternating direction method of multipliers (ADMM) is integrated into the MPC framework (Boyd et al., 2011; Bai et al., 2020). In addition, a data-driven split-ratio forecasting method is introduced to adapt the controller to time-varying turning movements. Overall, this paper combines lane-level traffic modeling, distributed MPC, ADMM-based optimization, and data-driven split-ratio forecasting to improve traffic signal control performance in urban networks. The main contributions are summarized as follows:

- In contrast to conventional road-based models, we propose a two-lane traffic model based on the store-and-forward framework, providing a more practical and accurate representation of the lane-level traffic flow propagation.
- We present a distributed MPC approach for traffic signal control in an urban network of interconnected intersections, and integrate ADMM to enhance real-time applicability and computational efficiency.
- We develop a data-driven method to forecast time-varying split ratios, enabling the controller to adapt to dynamic turning movements that are often neglected in existing approaches.

The rest of this paper is organized as follows. Section 2 presents the two-lane traffic model and formulates the traffic signal control problem. Section 3 introduces the distributed MPC framework and its integration with the ADMM algorithm. Simulation results are provided in Section 4, and in Section 5, we conclude the paper and discuss directions for future research.

2. PROBLEM FORMULATION

Consider a traffic network with N interconnected intersections. Each intersection is linked to eight incoming roads, where vehicles travel in the same direction on each road, as illustrated in Fig. 1. Each road contains two lanes: one dedicated to straight and right-turn movements, and the other to left-turn movements. To represent this network, we adopt a coupled-system framework in which each subsystem corresponds to an intersection and the four roads feeding into it. Specifically, the lanes marked by red arrows in Fig. 1 are associated with subsystem i, while those marked by green arrows belong to its neighboring subsystems. Each subsystem i is described by a local state vector $x_i \in \mathbb{R}^n$ and a local control input $u_i \in \mathbb{R}^m$, where $n = 8$ and $m = 4$. The state vector $x_i = [x_{i1}, \ldots, x_{i8}]^\top$ represents the number of vehicles in the eight incoming lanes of intersection i, while $u_i = [u_{i1}, \ldots, u_{i4}]^\top$ specifies the green times allocated to the four traffic signal phases.

The interactions among the N subsystems are modeled by a directed graph $\mathcal{G} = (\mathcal{V}, \mathcal{E})$, where the vertex set $\mathcal{V} = \{1, \ldots, N\}$ represents the set of subsystems and the edge set $\mathcal{E} \subseteq \mathcal{V} \times \mathcal{V}$ encodes their couplings. An edge $(j, i) \in \mathcal{E}$ with $i, j \in \mathcal{V}$ indicates that subsystem j directly affects subsystem i through a connecting road, making j a neighbor of subsystem i. The set of neighbors of subsystem i is denoted by $\mathcal{N}_i$, with $N_i = |\mathcal{N}_i|$.

The vehicle outflow from subsystem i is directly regulated by its local control input u_i. In contrast, the inflow into a subsystem is determined by the control inputs of its neighboring subsystems, resulting in coupled and interdependent dynamics across the network. The evolution of subsystem $i \in \mathcal{V}$ at time step $k \in \{0, 1, \ldots\}$ is described as

$$x_i(k+1) = x_i(k) - B_i(k)u_i(k) + C_i(k)z_i(k), \qquad (1)$$

where $B_i(k) \in \mathbb{R}^{n\times m}$ represents the outflow rate matrix, which can be obtained from road infrastructure measurements, and $B_i(k)u_i(k)$ denotes the number of vehicles exiting subsystem i at time step k. The term $C_i(k)z_i(k)$ captures the inflow of vehicles contributed by neighboring subsystems. Here, $C_i(k) \in \mathbb{R}^{n\times mN_i}$ is the matrix of transfer rates, and $z_i(k) \in \mathbb{R}^{mN_i}$ aggregates the control inputs of neighboring subsystems, given by

$$z_i(k) = \left[u_{j_1}^\top(k), \ldots, u_{j_{N_i}}^\top(k)\right]^\top, \qquad (2)$$

where $j_l \in \mathcal{N}_i$, $l = 1, \ldots, N_i$. The term $C_i(k)z_i(k)$ is explicitly expressed as

$$C_i(k)z_i(k) = \sum_{j_l \in \mathcal{N}_i} c_{j_l i}(k)u_{j_l}(k), \qquad (3)$$

where $c_{j_l i}(k)$, is the transfer rate from subsystem j_l to subsystem i. Since the transfer rates $c_{j_l i}(k)$ are influenced by multiple factors and directions, they are often difficult to measure directly and are treated as unknown parameters in this paper.

Remark 1. The traffic model proposed in Bianchin and Pasqualetti (2019) uses a single state variable to represent the number of vehicles on each road, which is then coupled with multiple control inputs. For example, as shown in

Fig. 1, combining the states x_{i1} and x_{i2} into a single state $\bar{x}_{i1}$ results in couplings with both control inputs u_{i1} and u_{i4}. Different from their work, the two-lane traffic model described in (1) decouples the state variables and control inputs, thus facilitating the integration of ADMM for efficient traffic signal optimization.

Unbalanced traffic flow distribution is a significant factor contributing to congestion, as it results in some lanes being overly congested while others remain underutilized. Inspired by Ru et al. (2023); Grandinetti et al. (2018), the goal of this work is to achieve a balanced vehicle density distribution across lanes. Specifically, we aim to achieve a local uniform vehicle density distribution for each lane and its downstream connections by designing appropriate control inputs for each subsystem. To this end, a distributed MPC method is proposed to allocate green times for traffic signals, mitigating congestion caused by uneven traffic flow distribution.

3. DISTRIBUTED MPC FOR TRAFFIC SIGNAL CONTROL VIA ADMM

This section presents a distributed MPC scheme to determine the green times of each signal phase across all intersections in the network. We start formulation of the distributed MPC problem, and then we describe how ADMM is integrated into the MPC framework to improve computational efficiency.

3.1 Distributed Traffic Signal Control via ADMM

A coordinated and scalable solution to the distributed MPC problem formulated in the previous subsection is achieved by employing ADMM, which decomposes the global objective into local subproblems that can be solved in parallel. To achieve a locally uniform vehicle density distribution for each lane relative to its downstream links (Ru et al., 2023; Grandinetti et al., 2018), we formulate the network-level cost function as the following form:

$$\min \sum_{i=1}^{N} \phi_i(k) = \sum_{i=1}^{N} \left(\sum_{m=1}^{8} \sum_{h=1}^{M} \Big(\rho_{im}(k+h) - \bar{\rho}_{im}(k+h) \Big)^2 \right. \\ \left. \sum_{h=1}^{M-1} u_i^\top(k+h) R_i u_i(k+h) \right), \tag{4a}$$

subject to

$$x_i(k+1) = x_i(k) - B_i(k) u_i(k) + C_i(k) z_i(k), \tag{4b}$$

$$\bar{\rho}_{im}(k+h) = \frac{1}{|N_{im}^+|} \sum_{jg \in N_{im}^+} \frac{x_{jg}(k+h)}{L_{jg}}, \quad h = 1, \ldots, M, \tag{4c}$$

$$\sum_{m=1}^{4} u_{im}(k+h) + Q_i = S, \quad h = 1, \ldots, M-1, \tag{4d}$$

$$u_{im}(k+h) \in [u_{\min}, u_{\max}], \quad h = 1, \ldots, M-1, \tag{4e}$$

where $x_{im}(k)$ and $u_{im}(k)$ denote the mth components of $x_i(k)$ and $u_i(k)$, respectively. The term $\bar{\rho}_{im}(k+h)$ represents the average density of the downstream lanes of lane im at the prediction step h, with L_{im} (and L_{jg}) denoting the lane length, and N_{im}^+ denoting the set of its downstream lanes of cardinality $|N_{im}^+|$. The weighting matrix $R_i = \mathrm{diag}(r_{i1}, r_{i2}, r_{i3}, r_{i4})$ is diagonal and positive definite, ensuring proper scaling of the two terms in (4a). Moreover, Q_i denotes the yellow-light duration at subsystem i, and S is the common cycle length across all intersections. The parameters $u_{\min}$ and $u_{\max}$ specify the minimum and maximum green times, respectively. The first term in (4a) penalizes the deviation of lane densities from their downstream averages, while the second term regularizes control efforts to enhance convergence.

By solving the optimization problem (4a) with constraints (4b)-(4e), one can derive the green time of each phase of all the intersections with the optimal performance for the entire network. However, the centralized optimization method involves massive data transmission and has high online computational complexity, which is impractical for multiple interconnected intersections. From the above analysis, an intersection belongs to only one subsystem after the traffic system decomposition. Hence, a distributed optimization framework for urban traffic signals is proposed. The optimization problem for each subsystem $i = 1, \ldots, N$ is presented as

$$\begin{aligned} \min \phi_i(k) = & \sum_{m=1}^{8} \sum_{h=1}^{M} \Big(\rho_{im}(k+h) - \bar{\rho}_{im}(k+h) \Big)^2 \\ & + \sum_{h=1}^{M-1} u_i{}^\top(k) R_i u_i(k), \\ \text{s.t.} \quad & \text{(4b)-(4e)}. \end{aligned} \tag{5}$$

Although the optimization problem of the whole network in (4a) can be decomposed into a distributed optimization problem in (5), it remains difficult to implement in large-scale urban networks, since solving (5) with constraints (4b)–(4e) directly may not satisfy real-time traffic control requirements (Lin et al., 2011; Farokhi et al., 2013). Note that, in our proposed two-lane traffic model, the state variables and control inputs are decoupled, which allows the optimization problem (5) to be further split into independent subproblems. Accordingly, the distributed MPC problem can be rewritten as

$$\min \phi_i(k) = \sum_{m=1}^{4} f_{im}\big(U_{im}(k)\big), \quad i = 1, \ldots, N, \tag{6}$$

subject to (4b)–(4e), where

$$\begin{aligned} f_{im}(U_{im}(k)) = & \sum_{h=1}^{M} \sum_{j \in \mathcal{L}_{im}} \Big(\rho_{ij}(k+h) - \bar{\rho}_{ij}(k+h) \Big)^2 \\ & + U_{im}^\top(k)\, r_{im}\, U_{im}(k), \end{aligned} \tag{7}$$

with $U_{im}(k) = \big[u_{im}^\top(k), \ldots, u_{im}^\top(k+M-1)\big]^\top$, r_{im} denoting the mth diagonal element of R_i, and $\mathcal{L}_{im}$ being the set of lanes associated with control group m.

Since the ADMM provides strong convergence properties and is well-suited for decomposable optimization problems with constraints, it is employed to solve (6) efficiently at each time step k. The detailed procedure is summarized in Algorithm 1. At every time step, each subsystem solves its optimization problem subject to constraints (4b)-(4e) after receiving the related information from its neighboring subsystems. The subsystem then shares the intermediate solution with its neighboring subsystems to enable solving their optimization problems. Finally, all the control inputs $U_i(k), i = 1, \ldots, N$ of the entire network can be obtained,

Algorithm 1 Distributed Signal Control via ADMM

Input: Maximum computation time $T_{\max}$; stopping threshold $\varepsilon_{\text{stop}}$.
Output: Control inputs $U_{i1}(k), U_{i2}(k), U_{i3}(k), U_{i4}(k)$.

for $i = 1, 2, \ldots, N$ **in parallel do**
  Initialize $s \leftarrow 1$, $t_i(k) \leftarrow 0$, and measure $x_i(k)$.
  while $\varepsilon^{(s)} \geq \varepsilon_{\text{stop}}$ **and** $t_i(k) \leq T_{\max}$ **do**
    Receive $U_j(k-1)$ and $y_j(k-1)$ from neighbors.
    Update $\mathcal{B}_i(k)$ and $\mathcal{C}_i(k)$.
    Solve the optimization problem

$$\min \mathcal{L}_\rho(U_{i1}(k), U_{i2}(k), U_{i3}(k), U_{i4}(k), \lambda)$$
$$= \sum_{m=1}^{4} f_{im}(U_{im}(k)) + \frac{\rho}{2}\|\vartheta(k)\|^2 + \lambda^\top \vartheta(k),$$

where

$$\vartheta(k) = \begin{bmatrix} \sum_{m=1}^{4} u_{im}(k+1) + Q_i - S \\ \sum_{m=1}^{4} u_{im}(k+2) + Q_i - S \\ \vdots \\ \sum_{m=1}^{4} u_{im}(k+M-1) + Q_i - S \end{bmatrix},$$

$$\lambda = [\lambda_1, \ldots, \lambda_{M-1}]^\top.$$

    Block updates:
    $U_{i1}^{(s)} \leftarrow \arg\min_{U_{i1}} \mathcal{L}_\rho\left(U_{i1}, U_{i2}^{(s-1)}, U_{i3}^{(s-1)}, U_{i4}^{(s-1)}, \lambda^{(s-1)}\right)$,
    $U_{i2}^{(s)} \leftarrow \arg\min_{U_{i2}} \mathcal{L}_\rho\left(U_{i1}^{(s)}, U_{i2}, U_{i3}^{(s-1)}, U_{i4}^{(s-1)}, \lambda^{(s-1)}\right)$,
    $U_{i3}^{(s)} \leftarrow \arg\min_{U_{i3}} \mathcal{L}_\rho\left(U_{i1}^{(s)}, U_{i2}^{(s)}, U_{i3}, U_{i4}^{(s-1)}, \lambda^{(s-1)}\right)$,
    $U_{i4}^{(s)} \leftarrow \arg\min_{U_{i4}} \mathcal{L}_\rho\left(U_{i1}^{(s)}, U_{i2}^{(s)}, U_{i3}^{(s)}, U_{i4}, \lambda^{(s-1)}\right)$,
    $\lambda^{(s)} \leftarrow \lambda^{(s-1)} + \rho \cdot \vartheta\left(U_{i1}^{(s)}, U_{i2}^{(s)}, U_{i3}^{(s)}, U_{i4}^{(s)}\right)$.
    Update $t_i(k)$.
    $\varepsilon^{(s+1)} \leftarrow \left\|\lambda^{(s)} - \vartheta\left(U_{i1}^{(s)}, U_{i2}^{(s)}, U_{i3}^{(s)}, U_{i4}^{(s)}\right)\right\|_\infty$.
    $s \leftarrow s+1$; send $U_i(k)$ and $y_i(k)$ to neighbors.
  end while
end for

and each subsystem i applies the first control of $U_i(k)$ as the optimal control.

4. SIMULATION STUDY

In this section, we conduct a realistic simulation study to evaluate the performance of the proposed two-lane traffic model and the distributed MPC scheme. We first outline the simulation setup and then introduce the benchmark control methods, as well as the performance metrics used for evaluation. Finally, the section concludes with a comparative analysis of simulation results.

4.1 Simulation Setup

The effectiveness of the proposed two-lane traffic model and distributed MPC scheme is evaluated through simulations on a six-intersection traffic network in Dalian, China, comprising 68 roads, as illustrated in Fig. 2. The traffic environment is simulated in VISSIM, while the control algorithms are implemented in Python. The simulation settings are as follows: the sampling period and the common cycle length of all intersections are both fixed at $S = 120$ seconds. The total simulation horizon is 7200 seconds, corresponding to 60 control intervals. The traffic demand is designed to replicate morning rush-hour conditions in Dalian, ranging from 300 to 800 vehicles per hour per road. For each traffic phase, the green time is constrained within $u_{\min} = 10$ seconds and $u_{\max} = 70$ seconds. In addition, the prediction horizon of the MPC controller is set to $M = 5$, meaning that five future time steps are considered in the optimization process.

(a) Geographic map of the selected intersections.

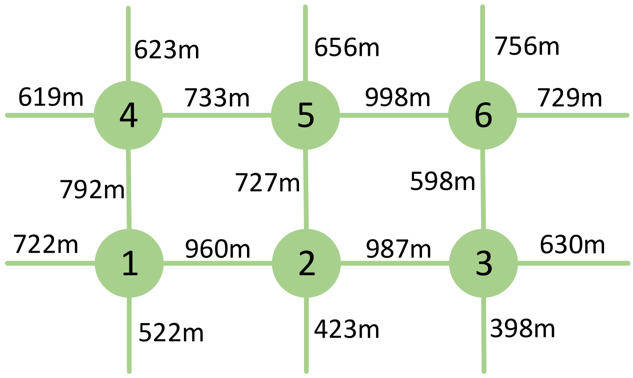

(b) Topological representation of the traffic network.

Fig. 2. Part of a traffic network of Dalian City, China.

We compare the proposed method with five baselines: FTC (Robertson, 1969), Max-Pressure, MFAPC (Ru et al., 2023), MPC-Road (Camponogara and De Oliveira, 2009), and MPC-CasADi. FTC uses fixed equal green times; Max-Pressure selects phases according to upstream-downstream pressure differences; MFAPC is a model-free distributed predictive controller; MPC-Road uses a road-level store-and-forward model; and MPC-CasADi solves the same MPC problem using CasADi without ADMM acceleration.

4.2 Performance Evaluation Metrics

The performance of different control strategies is evaluated using three key performance indicators: average density, average flow rate, and relative loss time. Specifically,

1) *Average Density:* It represents the mean vehicle density across all roads in the network. A lower value indicates less congestion and higher throughput, reflecting improved network performance.
2) *Average Flow Rate:* It characterizes the overall traffic condition of the network. It captures multiple aspects such as vehicle delays, travel speeds, and network throughput. Higher flow rates correspond to smoother traffic flow and reduced congestion.

Table 1. Performance metrics under different control strategies.

Control Strategy	Average Delay (sec)	Average Stops	Total Travel Time (min)	Average Computation Time (sec)
Proposed Method	105.164	3.129	937.502	1.323
MPC-CasADi	106.468	3.154	941.562	4.137
MFAPC	132.854	4.210	1018.436	0.972
Max-Pressure	148.372	4.856	1049.273	/
MPC-Road	164.235	5.264	1089.354	4.389
FTC	229.500	8.858	1345.288	/

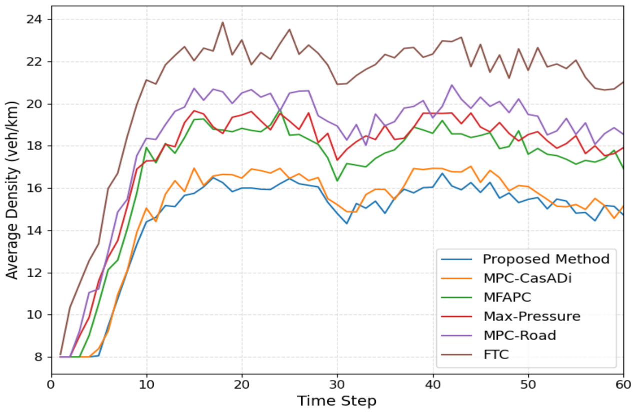

Fig. 3. Comparison of average vehicle density.

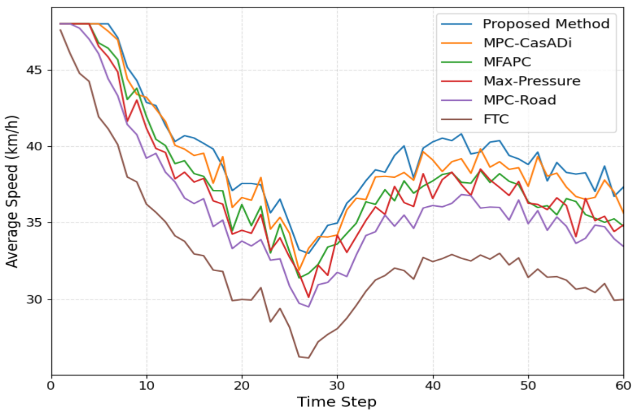

Fig. 4. Average vehicle speed in different control strategies.

3) *Relative Loss Time:* It measures the additional travel time experienced by vehicles compared to free-flow conditions. Larger values indicate more severe congestion and greater travel delays.

In addition to these three primary indicators, we also report several supplementary metrics, including the average travel time delay, average number of stops, total travel time, and average computation time. These indicators provide complementary insights into driving comfort, network-wide efficiency, and the real-time feasibility of different control strategies.

4.3 Simulation Results and Analysis

The comparison results are illustrated in Figs. 3–5 and summarized in Table 1. Specifically, Fig. 3 presents the evolution of the average density on the traffic network, Fig. 4 depicts the network-wide average vehicle speed, and

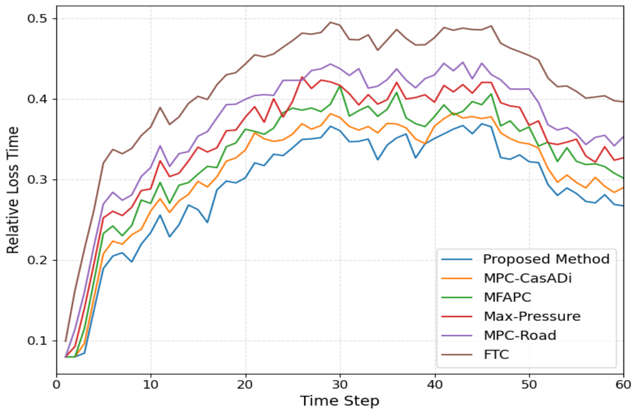

Fig. 5. Relative loss time in different control strategies.

Fig. 5 shows the relative loss time under each control strategy. The results show that the proposed method achieves lower per-lane average density, higher network-level speed, and smaller relative loss time compared with the other benchmark approaches. In addition, Table 1 shows that the proposed method achieves the best overall performance, yielding lower delays, fewer stops, shorter travel times, and reduced computation burden.

From these results, it is evident that the proposed MPC-ADMM strategy achieves the best overall performance across all evaluated metrics. It yields the lowest average delay, the fewest stops, the shortest total travel time, and the fastest computation time, demonstrating both strong control effectiveness and excellent real-time feasibility. Although MPC-CasADi attains similar control performance, its computation time is significantly higher due to the absence of ADMM-based acceleration. With the inclusion of MFAPC and Max-Pressure, the advantages of the proposed method become even more pronounced: MFAPC outperforms FTC and MPC-Road by leveraging adaptive pseudogradient updates but remains limited by its model-free structure, while Max-Pressure provides competitive performance under moderate traffic but degrades in oversaturated conditions. In contrast, both FTC and MPC-Road exhibit clearly inferior performance, with higher delays, more stops, and more severe congestion. These observations collectively confirm that the proposed two-lane traffic model, combined with the distributed MPC scheme solved via ADMM, provides substantial improvements over existing fixed-time, model-free, and model-based control methods.

5. CONCLUSION

In this paper, we proposed a two-lane traffic model for signal control that captures lane-level vehicle counts and turning movements, overcoming key limitations of traditional road-level formulations. Based on this model, we developed a distributed MPC framework for green-time optimization and integrated ADMM to improve real-time feasibility in interconnected traffic networks. A data-driven split-ratio forecasting method was further introduced to adapt the controller to time-varying turning behaviors. VISSIM simulations on a realistic six-intersection network in Dalian, China, demonstrated that the proposed approach improves both traffic efficiency and computational performance. Future work will investigate hierarchical control architectures to further enhance scalability in large-scale urban networks.

REFERENCES

Ba, Q., Savla, K., and Como, G. (2015). Distributed optimal equilibrium selection for traffic flow over networks. In *2015 54th IEEE Conference on Decision and Control (CDC)*, 6942–6947. IEEE.

Bai, T., Johansson, A., Johansson, K.H., and Mårtensson, J. (2023). Large-scale multi-fleet platoon coordination: A dynamic programming approach. *IEEE Transactions on Intelligent Transportation Systems*, 24(12), 14427–14442.

Bai, T., Li, A., Xu, G., Cassandras, C.G., and Malikopoulos, A.A. (2025). Routing guidance for emerging transportation systems with improved dynamic trip equity. In *2025 IEEE 64th Conference on Decision and Control (CDC)*, 1168–1173.

Bai, T., Li, S., and Zou, Y. (2020). Distributed MPC for reconfigurable architecture systems via alternating direction method of multipliers. *IEEE/CAA Journal of Automatica Sinica*, 8(7), 1336–1344.

Bang, H., Chalaki, B., and Malikopoulos, A.A. (2022). Combined optimal routing and coordination of connected and automated vehicles. *IEEE Control Systems Letters*, 6, 2749–2754.

Bianchin, G. and Pasqualetti, F. (2019). Gramian-based optimization for the analysis and control of traffic networks. *IEEE Transactions on Intelligent Transportation Systems*, 21(7), 3013–3024.

Boyd, S., Parikh, N., Chu, E., Peleato, B., Eckstein, J., et al. (2011). Distributed optimization and statistical learning via the alternating direction method of multipliers. *Foundations and Trends® in Machine learning*, 3(1), 1–122.

Camponogara, E. and De Oliveira, L.B. (2009). Distributed optimization for model predictive control of linear-dynamic networks. *IEEE Transactions on Systems, Man, and Cybernetics-Part A: Systems and Humans*, 39(6), 1331–1338.

Chalaki, B. and Malikopoulos, A.A. (2021). Time-optimal coordination for connected and automated vehicles at adjacent intersections. *IEEE Transactions on Intelligent Transportation Systems*, 23(8), 13330–13345.

Chalaki, B. and Malikopoulos, A.A. (2022). Optimal control of connected and automated vehicles at multiple adjacent intersections. *IEEE Transactions on Control Systems Technology*, 30(3), 972–984.

De Nunzio, G., Gomes, G., de Wit, C.C., Horowitz, R., and Moulin, P. (2015). Arterial bandwidth maximization via signal offsets and variable speed limits control. In *2015 54th IEEE Conference on Decision and Control (CDC)*, 5142–5148. IEEE.

De Oliveira, L.B. and Camponogara, E. (2010). Multi-agent model predictive control of signaling split in urban traffic networks. *Transportation Research Part C: Emerging Technologies*, 18(1), 120–139.

Farokhi, F., Shames, I., and Johansson, K.H. (2013). Distributed MPC via dual decomposition and alternative direction method of multipliers. In *Distributed Model Predictive Control Made Easy*, 115–131. Springer.

Grandinetti, P., Canudas-de Wit, C., and Garin, F. (2018). Distributed optimal traffic lights design for large-scale urban networks. *IEEE Transactions on Control Systems Technology*, 27(3), 950–963.

Le, V.A. and Malikopoulos, A.A. (2024). Distributed optimization for traffic light control and connected automated vehicle coordination in mixed-traffic intersections. *IEEE Control Systems Letters*, 8, 2721–2726.

Li, A., Bai, T., Chen, Y., Cassandras, C.G., and Malikopoulos, A.A. (2025). A cooperative compliance control framework for socially optimal mixed traffic routing. In *2025 IEEE 64th Conference on Decision and Control (CDC)*, 1162–1167.

Lin, S., De Schutter, B., Xi, Y., and Hellendoorn, H. (2011). Fast model predictive control for urban road networks via MILP. *IEEE Transactions on Intelligent Transportation Systems*, 12(3), 846–856.

Malikopoulos, A.A., Beaver, L.E., and Chremos, I.V. (2021). Optimal time trajectory and coordination for connected and automated vehicles. *Automatica*, 125(109469).

Robertson, D.I. (1969). TRANSYT method for area traffic control. *Traffic Engineering & Control*, 8(8).

Robertson, D.I. and Bretherton, R.D. (1991). Optimizing networks of traffic signals in real time–the SCOOT method. *IEEE Transactions on Vehicular Technology*, 40(1), 11–15.

Ru, X., Mei, C., Xia, W., and Shi, P. (2023). Distributed model-free adaptive predictive control of traffic lights for multiple interconnected intersections. *SCIENCE CHINA Information Sciences*, 66(9), 190209.

Sims, A.G. and Dobinson, K.W. (1980). The Sydney coordinated adaptive traffic (SCAT) system philosophy and benefits. *IEEE Transactions on Vehicular Technology*, 29(2), 130–137.

Tzortzoglou, F.N., Beaver, L.E., and Malikopoulos, A.A. (2024). A feasibility analysis at signal-free intersections. *IEEE Control Systems Letters*, 8, 2057–2062.

Yan, F., Tian, F., and Shi, Z. (2016). An extended signal control strategy for urban network traffic flow. *Physica A: Statistical Mechanics and Its Applications*, 445, 117–127.

Zaidi, A.A., Kulcsár, B., and Wymeersch, H. (2016). Back-pressure traffic signal control with fixed and adaptive routing for urban vehicular networks. *IEEE Transactions on Intelligent Transportation Systems*, 17(8), 2134–2143.